THE JOURNAL OF PHYSICAL CHEMISTRY C

Article

Cite This: J. Phys. Chem. C 2019, 123, 17010−17018

pubs.acs.org/JPCC

Atomistic and Mesoscopic Simulations of the Structure of CO_2 with Fluorinated and Nonfluorinated Copolymers

Armando Gama Goicochea[†,‡] and Abbas Firoozabadi*[,†,§]

[†]Reservoir Engineering Research Institute, Palo Alto, California 94301, United States

[‡]Departamento de Ingeniería Química y Bioquímica, Tecnológico de Estudios Superiores de Ecatepec, Ecatepec de Morelos, Estado de México 55210, Mexico

[§]Department of Chemical and Biomolecular Engineering, Rice University, Houston, Texas 77005, United States

Supporting Information

ABSTRACT: Viscosification of CO_2 by a low concentration of functional molecules is a prized task. It has two important applications. One is in fracturing of shale formation and the other is sweep efficiency improvement on the subsurface in hydrocarbon production. Toward that goal, we investigate the molecular structure of copolymers in CO_2 based on simulations at the atomistic and mesoscopic scales at various copolymer concentrations, pressure, and temperature. The effect of a small amount of water on the structure is also investigated. Three types of polymers are examined: fluorinated acrylate polymerized with styrene and two non-fluorinated copolymers. All of them, from experimental reports, show their effectiveness in increasing the viscosity of CO_2 by varying degrees. Our results show that there emerge three basic structures: dispersion in CO_2, formation of micelle-like aggregates, and interconnection of aggregates. In one of the three functional molecules, a small amount of water decreases the effective length and promotes the formation of aggregates. It is found that branched structures are favorable for solubility in CO_2 and that aggregation is promoted by intermolecular π-stacking. We expect this work to set the stage for molecular engineering in effective CO_2 viscosification.

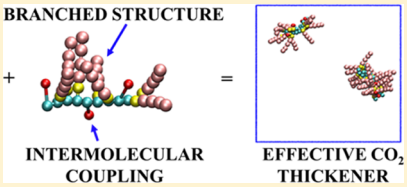

INTRODUCTION

The need to use effective and inexpensive fracturing fluids has focused on carbon dioxide (CO_2), which has numerous applications, driven by some attractive features, such as high mass diffusivity, nonflammability, and rapid recycling. It is innocuous, inexpensive in most cases, and relatively easy to produce. However, at the thermodynamic conditions of interest for many chemical engineering purposes, CO_2 viscosity is low, even though its density is liquid-like.[1] Low viscosity is unfavorable in fracking, where it reduces proppant carrying capacity, and in enhanced oil recovery, where it leads to low sweep of formation. One CO_2 viscosification process that has garnered interest is through the addition of small amounts of polymers and polymerizable surfactants forming reversed micelles.[2] Early work by Schurtenberger et al.[3] demonstrated that the viscosity of isooctane can be increased by a factor of 10^6 by formation of long reversed, cylindrically-shaped lecithin micelles. An entangled network formed at critical volume fractions of 0.1, which is a high concentration. The work of Schurtenberger and others[2,4] indicates that a small amount of water may be necessary for the mechanism to be operative, that is because the micelles become more stable[5−8] over time and the formation of a condensed phase by the surfactants is avoided;[9] without water, inverse micelles may not form.[7] Inverse micelle formation is not the only viscosification route—polymers long enough may interact with each other to form a network, which is an alternative mechanism.[10] For industrial applications, the surfactants and polymers must be environmentally friendly and highly effective at very low concentrations. Most efforts to viscosify CO_2 directly with the addition of polymers have focused on fluorine-based materials. The idea was pioneered by DeSimone, Guan, and Elsbernd,[11] who synthesized fluorinated copolymers of high molecular mass in supercritical CO_2. Huang and co-workers[10] increased the viscosity of CO_2 by a factor of 400 using copolymers made of styrene and fluoroacrylate monomers as direct viscosifiers at a relatively large concentration of 5 wt %. The polymers consist of a hydrocarbon backbone, with a monomer containing dangling branches of C_8F_{17} and other, shorter dangling branches of styrene.[10] The function of styrene is to promote intermolecular interactions between the aromatic rings in one copolymer chain and those in another (π-stacking). Fluorine increases the solubility in CO_2. Huang et al.[10] showed that a large increase in styrene content reduced the solubility of the copolymers, creating viscosity-reducing folded molecules rather than extended ones. Styrene content has an optimum value in the copolymer. High fluorine content (larger than 30% per copolymer) promotes intramolecular stackings, which are not desirable in viscosification. Fluorocarbons in the copolymer are known to have deleterious effects on the environment because the carbon−fluorine bond is very strong and hence the molecules do not easily degrade, in addition to being expensive.

Received: May 6, 2019
Revised: June 6, 2019
Published: June 11, 2019

DOI: 10.1021/acs.jpcc.9b04293
J. Phys. Chem. C 2019, 123, 17010−17018

A different double-tailed surfactant with a perfluorinated, seven-carbon chain, and the other chain with four hydrocarbons, both attached to a sulfate head was synthesized by Cummings et al.[12] The rationale for choosing this structure is based on the fact that the fluorinated chain is CO_2-philic, increasing solubility while the metal counterions help fine-tune micellar growth. Using small-angle neutron scattering data, Cummings et al. determined if the micelles are spherical. They found that rod-like reversed micelles increase the viscosity because there is more overlap between neighboring micelles. Yet, these surfactants still require fluorocarbon units to be soluble in CO_2. More recent experimental investigations of the viscosity increase by fluoroacrylate copolymers have shown that there is an optimal concentration of aromatic rings in these molecules.[13,14] Increasing it beyond a certain value leads to a reduction of the viscosity of CO_2. If the intramolecular interactions between aromatic rings increase, the chains shrink and the viscosity reduces. These studies indicate that fluorinated carbons are key ingredients for the improved solubility of the copolymers in CO_2. Even if the inimical environmental issues are avoided or reduced, there is still the high cost of formulations. Adsorption of fluorocarbons on rocks,[15,16] which has not been addressed in the past, provides another motivation to look for non-fluorine-based alternative viscosifiers. Polyfluoroacrylates have strong adsorption on sandstone and limestone,[15] therefore, they may not be effective in porous media.

The first report of viscosification of CO_2 with poly(1-decene) and poly(vinyl ethyl ether), two commercially available, nonfluorous polymers, was by Zhang et al.[17] They found that viscosity increases in CO_2 on the order of 14 times at polymer concentration up to 0.81 wt % and pressure up to 20.1 MPa. This large gain at low concentration was not confirmed later. No information was reported on the structure created by either of the polymers in CO_2. The solubility of both of these polymers in light crude oil and in CO_2 was studied by cloud point measurements and their interfacial tension, for pressure up to 15 MPa.[18] Al Hinai et al.[19] reported viscosity increases in CO_2 by P1D and PVEE in further investigations. Starting from a library of 26 nonfluorous containing polymers, they measured the solubility in CO_2 by the cloud point pressure, finding that up to 5 wt % of P1D and up to 2 wt % of PVEE were soluble in CO_2 at 55 MPa/377 K. The maximum viscosity gains were 277% for P1D (at 55 MPa/357 K/5 wt %) and 210% for PVEE (at 55 MPa/329 K/2 wt %). These increases are substantially lower than those reported by Zhang et al.[17] As for the mechanism that yields these improvements in viscosity, the authors attribute it to polymer expansion at increasing pressure because of an increase in solvent (CO_2) quality, although no measurements on the expansion were reported. Lastly, it is also claimed that increasing the side chain length of poly(vinyl alkyl ethers) may enhance the solubility in CO_2, but it does not improve the viscosity. No experimental data on the molecular structures of these two copolymers were provided.

To further understand these developments and to examine existing interpretations, we perform detailed computational simulations.[20,21] Simulations of surfactants in CO_2 have been performed by Salaniwal et al.[5,22,23] Their focus and that of others[24−26] was on reverse micelle structure, using CO_2 as a solvent. To the best of our knowledge, Sun et al.[13] reported the only study on fluorinated copolymers as thickeners of CO_2 by molecular simulations. They modeled chains made of vinyl benzoate (VBe) and heptadecafluorodecyl acrylate (HFDA) monomers, varying the molar ratios of VBe and HFDA, at a fixed concentration of eight copolymers either in vacuum or in 2000 CO_2 molecules. This concentration is higher than the solubility limit in CO_2.[27] From radial distribution functions (RDFs) of the C atoms in the copolymers and the C atoms in CO_2, they found that increasing the VBe content reduced the solubility in CO_2 and that the copolymer with the lowest VBe content (0.13 molar ratio) was the most soluble in CO_2. However, the RDFs of C−C pairs in VBe groups show that the strongest correlation is for the copolymers with 0.33 molar ratio of VBe, which are the best CO_2 thickeners from their experiments. Because VBe has aromatic rings, it can form π-stackings, which is the aggregation mechanism proposed by Sun et al.[13] Separate effects from intramolecular and intermolecular π-stacking were not studied.

In this work, we present an integral approach, whereby the details of microscopic interactions between viscosifying molecules and CO_2 are investigated from atomistically detailed molecular dynamics (MD) simulations. The need to model several concentrations and thermodynamic conditions for relatively large systems in a timely fashion calls for the use of accurate mesoscale techniques. One of the most successful among such techniques is dissipative particle dynamics (DPD).[28,29] Its simple interparticle interactions allow for the integration of the equations of motion with time steps of the order of picoseconds,[30] some being 3 orders of magnitude larger than the time step used in most atomistic-level simulations.[20] Complementing the results from the atomistic simulations with DPD simulations constitute a robust approach that, as we shall show, provides powerful insights into the association and thickening mechanisms of the copolymers studied here. We proceed by investigating in detail the structure imparted by P1D, PVEE, and HFDA in CO_2. The consequences of adding a small amount of water are also researched by atomistic and mesoscale numerical simulations, under conditions as in experiments. This is the first numerical simulation of the nonfluorinated copolymers and also the first multiscale approach, to the best of our knowledge. We aim at understanding the association mechanisms between these molecules that give rise to the collective behavior of solubility in CO_2. The results can guide the engineering of new thickeners that can enhance CO_2 viscosity to a desired level.

The structures of the three molecules studied in this work are shown in Figure 1. We start with P1D and PVEE, in Figure 1a,b, respectively. The HFDA molecule is shown in Figure 1c. It is a copolymer made of fluorinated carbons with styrene rings using the concentration that is known from experiments to be the most effective, at 70% fluorinated carbons and 30% styrene rings. To compare with the published data, P1D and PVEE (Figure 1a,b, respectively) were modeled at concentrations of 1.5 wt % (at 53 MPa/358 K). The HFDA molecule (Figure 1c) was modeled in CO_2 at 2 wt % concentration and at 34.4 MPa/298 K.

RESULTS AND DISCUSSION

The structure of a single P1D copolymer in CO_2 at 53 MPa/358 K is shown in Figure 2a; P1D branches extend into the surrounding CO_2 (for clarity, CO_2 molecules are not shown). The leading spatial correlations from the RDFs are presented in Figure 2b. H-bonds are formed between oxygen in CO_2 and hydrogen in P1D (dashed red line in Figure 2b), as well as that

DOI: 10.1021/acs.jpcc.9b04293
J. Phys. Chem. C 2019, 123, 17010−17018

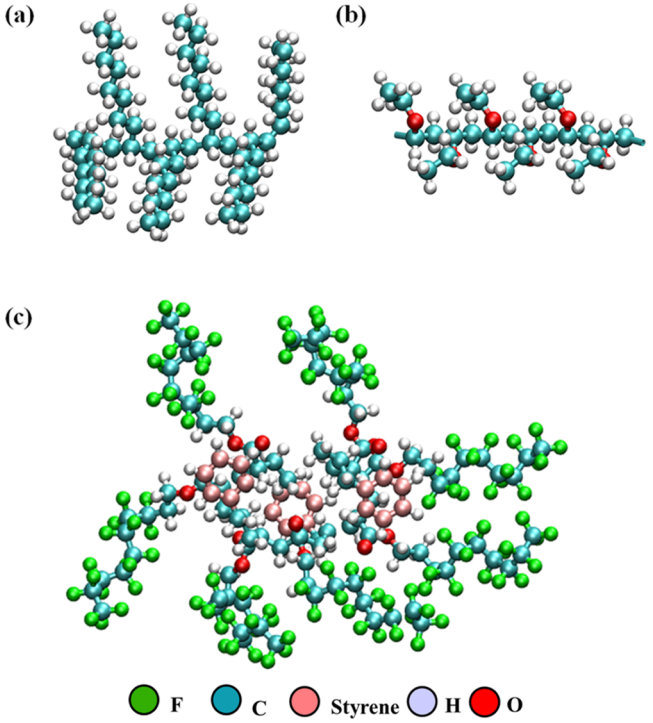

Figure 1. Chemical structure of CO_2 viscosifiers. (a) Poly(1-decene), $[CH_2CH[(CH_2)_7CH_3]]_n$, with n = 6. (b) Poly(vinyl ethyl ether), $[CH_2CH(OC_2H_5)]_n$. with n = 53. A section of the molecule with six monomers is shown, for clarity. (c) Polyheptadecafluorodecyl acrylate polymerized with styrene, $C_{25}H_{40}O_2(C_9F_{19})_x(C_6H_5)_y$ (HFDA), with x = 7, y = 3.

between the C atom in CO_2 and hydrogen in P1D (dotted blue line in Figure 2b).

In Figure 2c, one finds a snapshot of a single PVEE molecule at 53 MPa/358 K in 2600 molecules of CO_2. The structure in Figure 2c shows a relatively extended spatial conformation of the linear PVEE chain, indicating its solubility in CO_2 at the simulated pressure and temperature. The RDFs in Figure 2d show that the solubility of PVEE in CO_2 is driven by the same leading correlations as in P1D, that is, those between O in CO_2 with H in PVEE and C in CO_2 with H in PVEE. Next comes the RDF of C in CO_2 with O in PVEE (solid black line in Figure 2d). It is followed by the one between O in CO_2 and O in PVEE (dashed red line in Figure 2d). Comparison of Figure 2b,d reveals a stronger H-bond correlation in P1D (O in CO_2 with H in P1D) than the O-bond correlation in PVEE (O in PVEE with C in CO_2). This prediction is in agreement with the measurements of Al Hinai et al.,[19] who found that the solubility of P1D is higher than in PVEE at the same pressure and temperature.[19] The area under the RDF between O in CO_2 and H in P1D is about 5% larger than that under the RDF between O in CO_2 and H in PVEE. Also, the area under the RDF for C in CO_2 and H in P1D is 5% higher than that under C in CO_2 and H in PVEE RDF. It is the branched structure of P1D which lends its higher solubility in CO_2; additional comparisons can be found in Figures S6 and S7 of the Supporting Information.

The structural information from atomistic simulations of the molecule of HFDA in CO_2 at 34 MPa/298 K is shown in Figure 2e,f. The snapshot in Figure 2e shows the fluorinated branches of HFDA extending into CO_2, providing a high degree of solubility. Figure 2f presents the RDFs of various atoms of the HFDA molecule with CO_2. The strongest correlation is between fluorine and the oxygen atoms in CO_2. It is followed closely by that of the oxygen atoms in HFDA with the carbon atoms in the CO_2 molecules. Next is the RDF of fluorine with carbon in CO_2. Experimental data[10] show that the aromatic rings in the fluorinated carbons help increase the

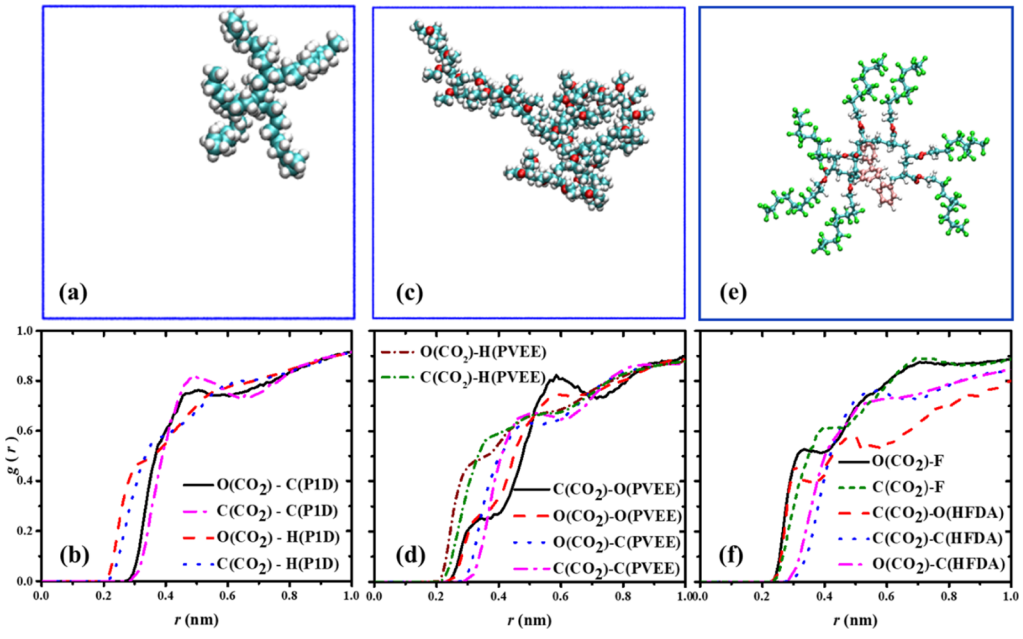

Figure 2. Snapshots of the structure and RDFs from atomistic simulations. (a) Structure of a single P1D molecule in 600 CO_2 molecules at 53 MPa/358 K. (b) RDFs between the atoms in CO_2 and in P1D. (c) Structure of a single PVEE molecule in 2600 CO_2 molecules at 53 MPa/358 K. (d) RDFs between the atoms in CO_2 and in PVEE. (e) Structure of a single molecule of HFDA in 2600 CO_2 molecules, at 34 MPa/298 K. (f) RDFs between the atoms in HFDA and in CO_2. CO_2 molecules are not shown in (a,c,e) for clarity.

DOI: 10.1021/acs.jpcc.9b04293
J. Phys. Chem. C 2019, 123, 17010−17018

viscosity of CO_2 substantially. It is speculated that this occurs because the HFDA + styrene copolymer couples through π-stackings[31,32] with other molecules of the same type in CO_2.[10,13,14]

In many processes where polymers are used, water is almost unavoidable, but its concentration may be low. Water uptake in the polymer and surfactant inverse micelles may help increase the viscosity of CO_2, as found by Cummings et al.[12] We investigate the effect of water in the structure of the copolymers in CO_2. Figure 3a shows a snapshot of PVEE in

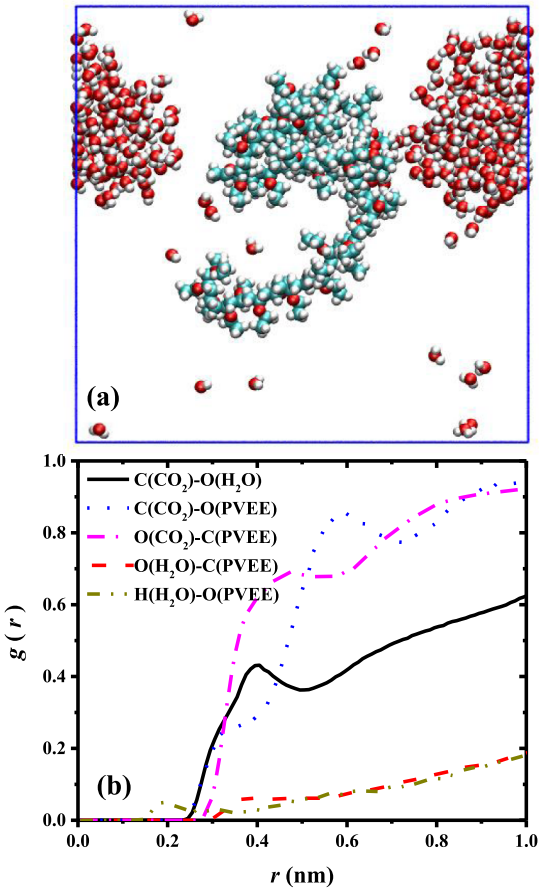

Figure 3. (a) Snapshot from atomistic simulations of the structure of one PVEE molecule with 350 water molecules in 2600 CO_2 molecules at 53 MPa and 358 K; CO_2 molecules are not shown for clarity. (b) RDFs, $g(r)$, between the atoms in water and PVEE with CO_2. Water concentration is 13 wt %.

CO_2, with water at a concentration of 13 wt % and 53 MPa/358 K. This is well above the solubility of water in CO_2 (0.55 wt % at 34.5 MPa/348 K[33]) under the given conditions, which is why most water molecules are seen forming a droplet. However, when the number of water molecules, that are not part of the droplet, are counted and averaged over the production period of the simulation, we obtain a water concentration of 0.46%. This is in reasonable agreement with the water solubility in CO_2 data.[33] Some of the water molecules associate with the PVEE chain, promoting its folding, which is more pronounced with water than without it (Figures 2c and 3a).

The spatial association taking place in PVEE when water is added to the system can be examined from the RDFs shown in Figure 3b. The smallest of all five RDFs shown in the figure are those between water and PVEE, but the fact that they are nonvanishing at very small distances may contribute to PVEE folding. Additionally, there is solubility of water in CO_2 at these conditions (53 MPa/358 K). This can be learned not only from the snapshot in Figure 3a but more importantly from the solid line in Figure 3b. The latter is the RDF between the oxygen atoms in water and the carbon atoms in CO_2 molecules. It is nonvanishing at the smallest distances (about 2.5 Å) and has a maximum around 4 Å. Hydrogen bond formation at distances smaller than 2 Å between H in water and O in PVEE is shown by the dash-dot-dot line (in dark yellow) in Figure 3b. The conclusion extracted from Figure 3 is that water associates with PVEE, giving rise to its folding. This feature is expected to influence the viscosity of CO_2 because interconnected, folded PVEE molecules have more inertial resistance to flow than single molecules. The structure of P1D and HFDA in CO_2 appears to be unaffected by the addition of water; the results are included in the Supporting Information for brevity. The fluorinated HFDA contrasts with the short, dichain semifluorinated surfactants[12] that form inverse micelles with water. These surfactants have a cation head and a hydrophobic tail, which are crucial for the formation of micelles and which HFDA does not have. Figures 2b,d, and 3b show weak but detectable formation of blue-shifted hydrogen bonds under the conditions of our simulations. This finding is in agreement with the work of Trung and collaborators,[34] who study complexes of carbonyls and thiocarbonyls with CO_2. They conclude that bond contraction and blue shift in frequency in the C−H bond are determined by its polarization.

We now present the results from DPD simulations, to capture the mesoscale structuring of CO_2 with copolymers. Before modeling the three copolymers at the mesoscopic scale, we have examined the DPD force field by choosing the amplitude of the conservative, nonbonding DPD force given by[28,29]

$$\vec{F}_{ij}(\vec{r}_{ij}) = a_{ij}[1 - |\vec{r}_{ij}|/r_C]\hat{r}_{ij} \quad (1)$$

where $\vec{F}_{ij}$ is the force between the centers of mass of particles i and j, which are separated by the relative position vector $\vec{r}_{ij}$, whose magnitude is $|\vec{r}_{ij}|$; the unit vector is $\hat{r}_{ij} = \vec{r}_{ij}/|\vec{r}_{ij}|$. The force is identically equal to zero for relative distances larger than the cutoff radius, r_C. The amplitude of this force is given by the constant a_{ij}, which is obtained from the solubility parameters of the substances of type i and j in the interaction.[30] Based on the solubility parameter data,[35−37] we calculated the density of CO_2, the interfacial tension between water and CO_2, and between PVEE/CO_2 and P1D/CO_2. The predictions are in agreement with experiments,[18,38] confirming the essential correctness of our model. Full details including these verifications can be found in the Supporting Information.

The coarse-grained mapping of the copolymers is shown in Figure 4, along with the atoms grouped in each bead. Figure 5a shows the P1D molecules are dispersed in CO_2, at 1.5 wt % and at 53 MPa/358 K. They move freely and have many intermolecular collisions with CO_2 and with other P1D molecules, which increases their translational entropy. This mobility is a feature that can viscosify CO_2.[12]

The concentration profiles in Figure 5b show virtually no aggregation between the P1D copolymers at 53 MPa/358 K. They are uniformly distributed all over the simulation box, as an indication of their solubility in CO_2. The RDF of $CH_2CH_2CH_2$ with CO_2 (dash-dot-dot, olive line in Figure

DOI: 10.1021/acs.jpcc.9b04293
J. Phys. Chem. C 2019, 123, 17010−17018

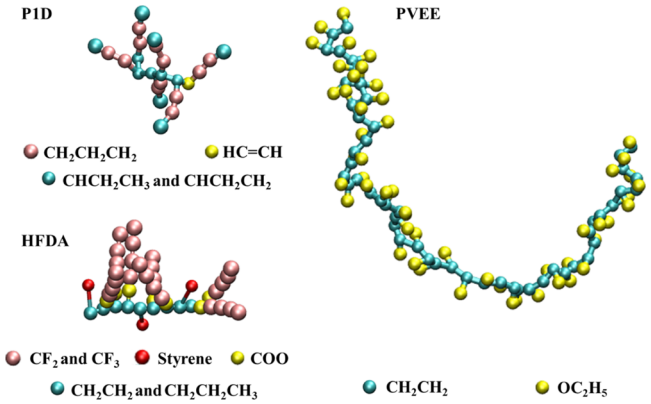

Figure 4. Coarse-grained (DPD) models of copolymers P1D, PVEE, and HFDA. The chemical composition of different beads is provided.

5c) is the closest to the one for CO_2 with itself (solid black line in Figure 5c). These are the beads that make up the branches of P1D. The RDF shows $CH_2CH_2CH_2$ beads have the strongest effect on the solubility of P1D in CO_2, confirming what was found at the atomistic scale (see Figure 2). The average end-to-end distance (R_e) of P1D shown in Figure 5d, is about 2 nm during the simulation, indicating that there is very little bending of the copolymer molecules.

In Figure 6a, there is a snapshot of a typical PVEE configuration; some isolated chains are dispersed in the medium but most are aggregated in networks. The PVEE concentration profiles in Figure 6b display agglomeration close to the center of the box, but are otherwise uniformly distributed in it. The RDFs for this system and the PVEE chains' average R_e are shown in Figure 6c,d, respectively. The RDFs show that the OC_2H_5 bead of PVEE interacts preferentially with CO_2. R_e is the effective length. Applying the well-known scaling law,[39] $R_e = bn^{\nu}$, where b is the monomer size, ν is Flory's exponent, and n the polymerization degree, we find the Flory exponent is $\nu = 0.56 \pm 0.06$. This exponent is less than the expected value for good solvent conditions ($\nu = 0.588$)[40] but is close to it; hence, CO_2 acts as a good solvent at 53 MPa/358 K when the concentration is 1.5 wt %.

The effect of water in the PVEE/CO_2 system at 53 MPa/358 K is shown in Figure 7; the water concentration is 0.4 wt %, well within the solubility margin.[33] This is consistent with our results, as water beads are seen dispersed in the box, see Figure 7a. Some water beads are associated with PVEE chains, yielding their partial folding and aggregation. The PVEE concentration profiles in Figure 7b follow closely one another because the distance between the two bead types in PVEE is very small. The maxima in the water beads' profiles appear where there are maxima in the PVEE beads' profiles because the former are "adsorbed" by the latter.

The oxygen-containing bead in PVEE (OC_2H_5, short dash dark yellow line) drives the folding of the polymer, as concluded from the RDFs in Figure 7c. However, Figure 7d demonstrates that the chains are still relatively extended. The contraction in R_e induced by the addition of water is about 20% with respect to the waterless case.

We complete our study with the fluorinated surfactant, HFDA in CO_2. To compare with the published data,[10] we modeled systems at 34 MPa/298 K for concentrations in the range 1−5 wt %. Panels 8a−e show snapshots of the HFDA molecules at increasing concentration. The HFDA molecules are seen to form aggregates that are stable over time. The

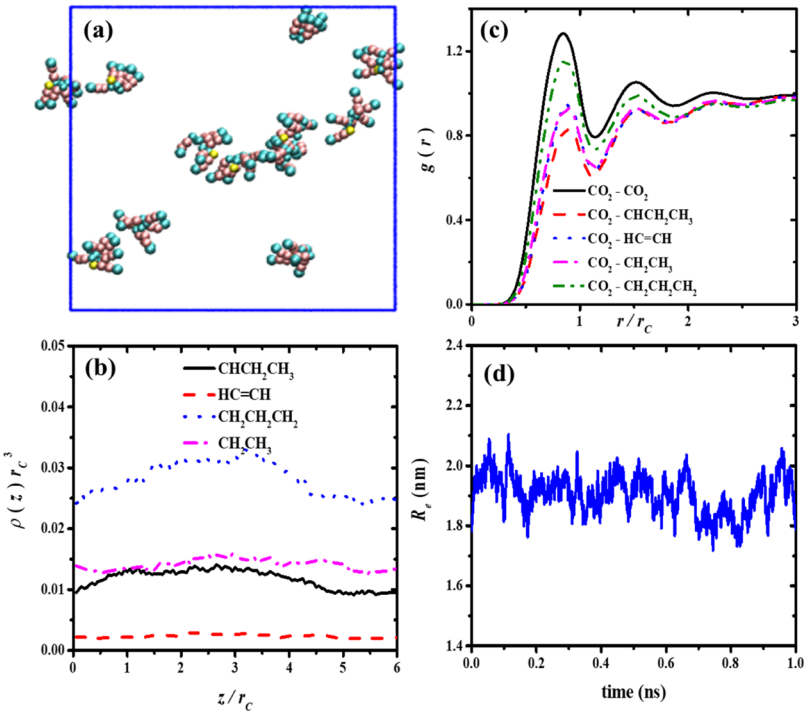

Figure 5. (a) Snapshot from the *xy* plane of the structure of 12 molecules of P1D with 15 ;011 CO_2 molecules at 35 MPa/358 K and concentration 1.5 wt %. The CO_2 molecules are not shown for clarity. (b) Concentration profiles of each bead type along the *z*-direction of the simulation box. (c) RDFs of the beads of P1D. The cutoff radius is r_C = 6.48 Å. (d) Average end-to-end distance of the P1D polymer in the last 1 ns of the production of the simulations. The box of this DPD simulation has dimensions 19 × 19 × 4 nm^3.

DOI: 10.1021/acs.jpcc.9b04293
J. Phys. Chem. C 2019, 123, 17010−17018

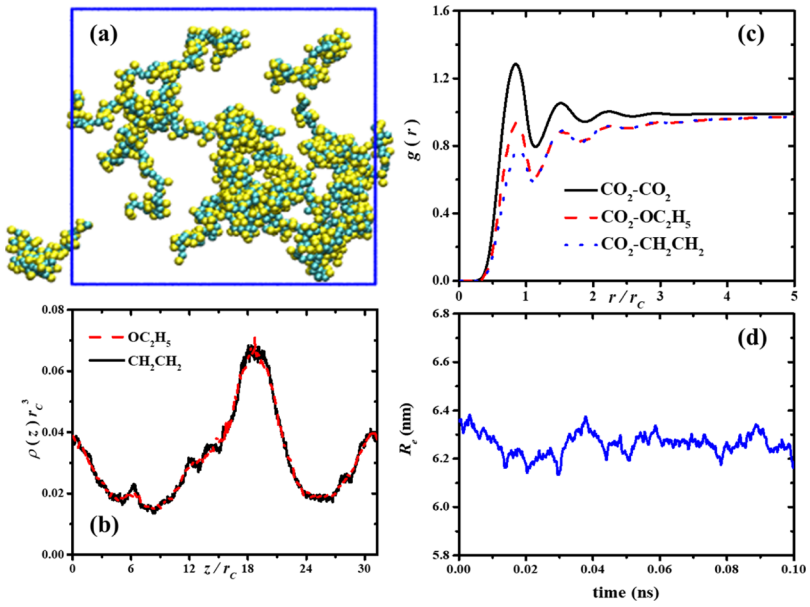

Figure 6. (a) Intermolecular association of 18 PVEE molecules with 90 ;092 molecules of CO_2 at 53 MPa/358 K and concentration 1.5 wt %. CO_2 molecules are not shown, for clarity. (b) Concentration profiles of the beads. (c) RDFs of the beads. (d) Average end-to-end distance of the PVEE chains in the last 100 ps of production time. The cutoff radius is r_C = 6.48 Å. The box volume in these DPD simulations is 20.3 × 20.3 × 20.3 nm^3.

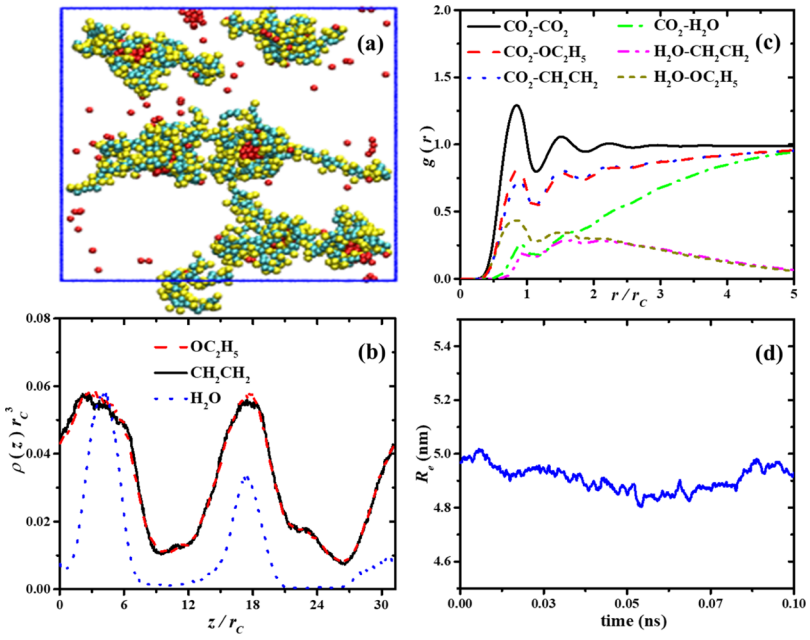

Figure 7. (a) Aggregation state of 18 molecules of PVEE (at 1.5 wt %) with 360 water beads (at 0.4 wt %, red monomers) in 89 ;732 CO_2 molecules at 53 MPa/358 K. CO_2 molecules are not shown, for clarity. (b) Bead concentration profiles. (c) RDFs of the beads. The H_2O−CH_2CH_2 and H_2O−OC_2H_5 RDFs are divided by 50. (d) Average R_e distance of the PVEE chains in the last 100 ps of the production time of the simulations. The cutoff radius is r_C = 6.48 Å. The box volume of these DPD simulations is 20.3 × 20.3 × 20.3 nm^3.

fluorinated branches (pink beads in Figure 8) extend into the medium, just as in P1D (Figure 5a). The snapshot in Figure 8e shows the structure of the HFDA at 5 wt %, in a box larger than that in 8a−d. Aggregates of few molecules are formed, showing that this association is size-independent. The concentration profiles of the beads that make up HFDA are presented in Figure 8f, for 3 wt % concentration, as a typical example. Qualitatively similar profiles are found for other concentrations. Even though HFDA molecules aggregate strongly, the profiles in Figure 8f show that they sample most of the simulation box evenly, producing relatively uniform concentration profiles.

Figure 9 shows the contributions from the intramolecular and intermolecular π-stackings. The RDFs in Figure 9a show that the fluorinated carbon units follow closely the RDF of CO_2, specially at short distances. This is a consequence of the high solubility of those beads in CO_2, promoted by fluorine, but the strongest spatial correlation is found between the styrene beads.[31,32] The associating mechanism between the copolymers is π-stacking interaction (see Figure 9b), as found by Sun et al.[13] using MD simulations of VBe/HFDA, which

DOI: 10.1021/acs.jpcc.9b04293
J. Phys. Chem. C 2019, 123, 17010−17018

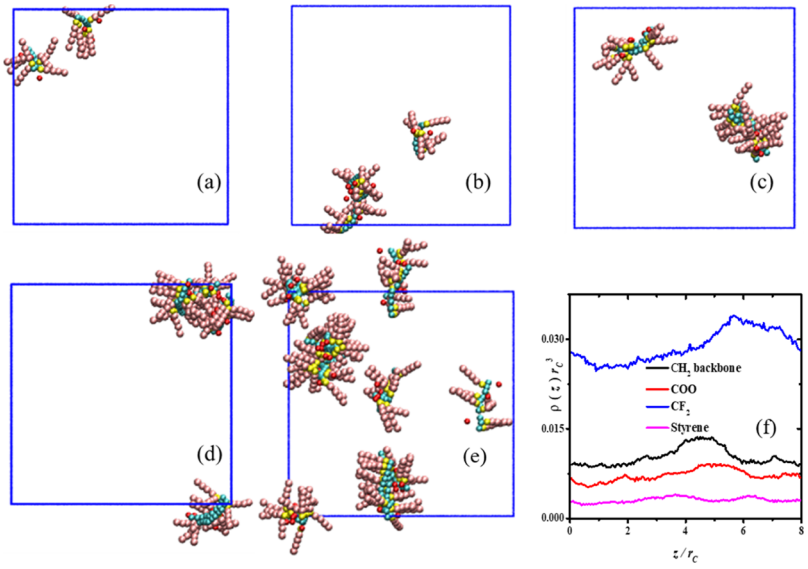

Figure 8. *xy*-plane snapshots (a–e) of the HFDA copolymer at 34 MPa/298 K and different concentrations after 20 ns during the production phase. (a) 1 wt %, 2 HFDA, and 17 ;404 CO_2 molecules; (b) 2 wt %, 4 HFDA, and 17 ;308 CO_2 molecules; (c) 3 wt %, 6 HFDA, and 17 ;212 CO_2 molecules; (d) 4 wt %, 8 HFDA, and 17 ;212 CO_2 molecules; (e) 5 wt %, 20 HFDA, and 34 ;040 CO_2 molecules; (f) bead concentration profiles for concentration 3 wt %. The box volume is 17.5 × 17.5 × 5.2 nm^3 for (a–d) and (f) 24.74 × 24.74 × 5.2 nm^3 for (e), all are DPD simulations.

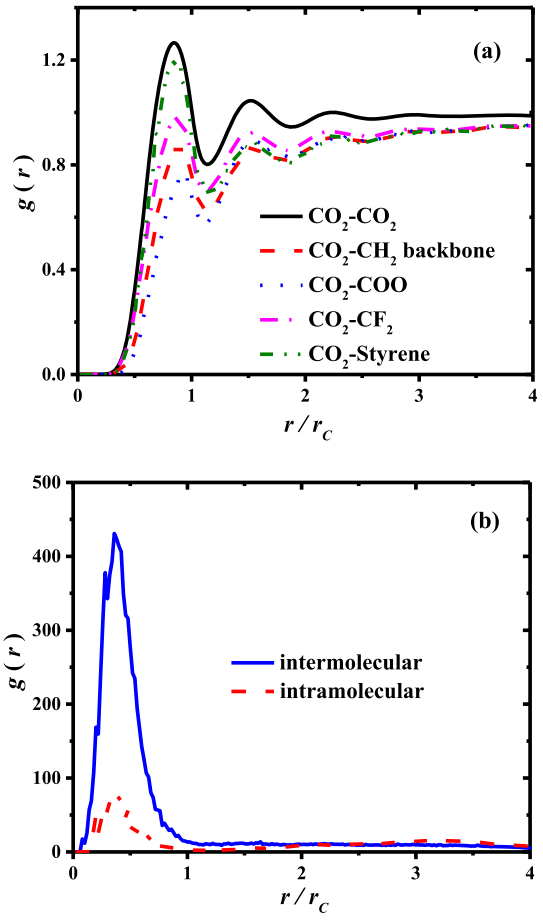

Figure 9. (a) RDFs of the beads that make up the HFDA copolymer. The box contains two HFDA molecules in 17 ;404 CO_2 molecules at 34 MPa/298 K, at concentration 1 wt %. As a reference, the CO_2–CO_2 RDF is also included. (b) RDF between styrene beads, responsible for π-stackings. The cutoff radius is r_C = 6.48 Å. The box volume of these DPD simulations is 17.5 × 17.5 × 5.2 nm^3.

has aromatic rings. The aggregates seen in the snapshots in Figure 8 are driven by intermolecular π-stackings, not by intramolecular; the latter do not contribute to CO_2 viscosification. As the number of aromatic rings increases in a molecule, we may expect more intramolecular stacking which does not promote the viscosification observed experimentally, as discussed in the Introduction.

Our simulations show that branching improves the dispersion of the polymers in CO_2, while aromatic rings induce aggregates formed by π-stackings, which change the structure. These opposite features may help explain the data plotted in Figure 10.[10,19] The solubility of the nonfluorinated polymers grows logarithmically with increasing polymer concentration, while for HFDA, it grows exponentially, see Figure 10a. Remarkably, those are also the trends found in their viscosity gains, Figure 10b. When these tendencies are put in the context of our findings, one concludes that branching must be accompanied by an intermolecular coupling mechanism, such as π-stacking, in the search for better CO_2 viscosifiers.

CONCLUSIONS

Detailed atomistic and mesoscale numerical simulations of experimentally relevant CO_2 viscosifiers are undertaken to investigate the structure and understand their thickening mechanisms. Our results show that P1D disperses well in CO_2, indicating good solubility for a fluorine-free polymer. PVEE molecules prefer to associate in a network-like fashion, with the chains enjoying ample freedom to move around, yet creating dynamical entanglements. The fluorinated HFDA forms aggregates with other molecules of its kind mostly through π-stackings, with the fluorinated carbon branches extending into CO_2 because of high solubility. However, it is not viable as a viscosifier for environmental and economic reasons. Also, recent experiments show fluorinated copolymers adsorb strongly on porous media, reducing their effectiveness in enhanced oil recovery.[15] The addition of water in relatively small concentrations produces partial folding of the PVEE

DOI: 10.1021/acs.jpcc.9b04293
J. Phys. Chem. C 2019, 123, 17010–17018

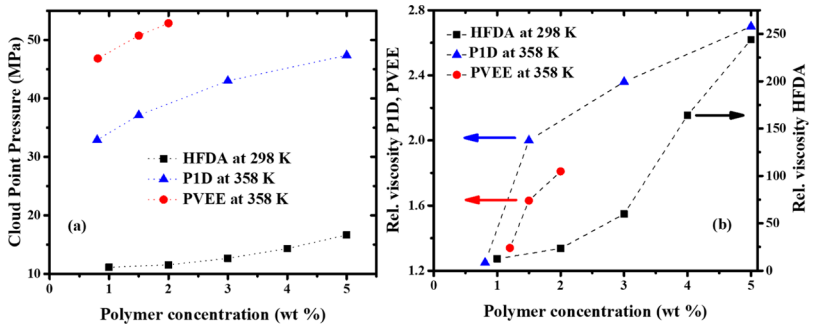

Figure 10. (a) Solubility of the P1D/PVEE/HFDA copolymers and (b) relative viscosity, in CO_2. Data for HFDA are from Huang et al.[10] and data for P1D and PVEE are from Al Hinai et al.[19]

chains, which form complex, elongated shapes. This aspect is expected to affect the viscosification of CO_2 by this copolymer. We find that the branched structure of P1D is what makes it more soluble in CO_2 than PVEE and it is driven by H bonding with O in CO_2. However, experiments show that P1D viscosifies CO_2 considerably less than the fluorinated HFDA,[10,19] which means that solubility is a necessary but not sufficient condition for viscosification. We find that the aggregation state can be very different even if the molecules are soluble in CO_2, as P1D and HFDA, which influences their viscosity. We believe this work has set the stage for molecular engineering of functional molecules as CO_2 viscosifiers.

MODELS AND METHODS

All the MD simulations are carried out using the LAMMPS[41] simulation suite with the polymer consistent force field plus (PCFF+).[42] The procedure starts with simulations in the *NVT* ensemble (at constant number of atoms, N, volume, V, and temperature, T), for the relaxation period of 10 ns using a time step equal to 1 fs. Afterward, simulations in the *NPT* (at constant pressure) ensemble are performed for at least an additional 20 ns, all under periodic boundary conditions. Full details are included in the Supporting Information.

In the mesoscale modeling, DPD simulations are performed in the *NVT* ensemble. A coarse-graining degree equal to three water molecules per DPD bead is used; one CO_2 molecule is coarse-grained in one DPD bead. The beads are joined by harmonic springs whose parameters k_0 and r_0 have been successfully investigated.[43] The simulations are performed in reduced units, so that temperature, mass, and cutoff radius are $T = m = r_C = 1$, respectively. The time step used is $\delta t = 0.03$ and the global numerical density is always kept equal to 3, to ensure that the DPD equation of state remains invariant with respect to changes of interaction parameters. To dimensionalize energy, length, and time, we use the thermal energy at room temperature, k_BT, r_C = 6.48 Å, δt = 3 ps, as it is appropriate for a coarse-graining degree equal to three. The simulations are run for up to 100 ns, with the first half used for reaching equilibrium and the rest for the production phase.

ASSOCIATED CONTENT

Supporting Information

The Supporting Information is available free of charge on the ACS Publications website at DOI: 10.1021/acs.jpcc.9b04293.

Full details of atomistic simulations; structural properties of CO_2 with water and the fluorinated copolymer; structural properties of water with P1D at the atomistic level; full details of DPD simulations; structural properties of P1D and PVEE at 20 MPa/313 K with and without water; and solubility determination (PDF)

AUTHOR INFORMATION

Corresponding Author

*E-mail: Abbas.Firoozabadi@rice.edu, af@rerinst.org.

ORCID

Abbas Firoozabadi: 0000-0001-6102-9534

Notes

The authors declare no competing financial interest.

ACKNOWLEDGMENTS

The authors would like to thank the member companies of the RERI for their support. A.G.G. would like to thank S. Tesson for discussion and CONACYT for a sabbatical scholarship.

REFERENCES

(1) Bachu, S. Sequestration of CO_2 in Geological Media in Response to Climate Change: Road Map for Site Selection Using the Transform of the Geological Space into the CO_2 Phase Space. *Energy Convers. Manage.* **2002**, *43*, 87−102.

(2) Goetheer, E. L. V.; Vorstman, M. A. G.; Keurentjes, J. T. F. Opportunities for Process Intensification Using Reverse Micelles in Liquid and Supercritical Carbon Dioxide. *Chem. Eng. Sci.* **1999**, *54*, 1589−1596.

(3) Schurtenberger, P.; Scartazzini, R.; Magid, L. J.; Leser, M. E.; Luisi, P. L. Structural and Dynamic Properties of Polymer-Like Reverse Micelles. *J. Phys. Chem.* **1990**, *94*, 3695−3701.

(4) Hoefling, T. A.; Enick, R. M.; Beckman, E. J. Microemulsions in Near-Critical and Supercritical Carbon Dioxide. *J. Phys. Chem.* **1991**, *95*, 7127−7129.

(5) Salaniwal, S.; Cui, S. T.; Cummings, P. T.; Cochran, H. D. Self-Assembly of Reverse Micelles in Water/Surfactant/Carbon Dioxide Systems by Molecular Simulation. *Langmuir* **1999**, *15*, 5188−5192.

(6) Lu, L.; Berkowitz, M. L. Molecular Dynamics Simulation of a Reverse Micelle Self Assembly in Supercritical CO_2. *J. Am. Chem. Soc.* **2004**, *126*, 10254−10255.

(7) Khoshnood, A.; Firoozabadi, A. Polar Solvents Trigger Formation of Reverse Micelles. *Langmuir* **2015**, *31*, 5982−5991.

(8) Liu, B.; Tang, X.; Fang, W.; Li, X.; Zhang, J.; Zhang, Z.; Shen, Y.; Yan, Y.; Sun, X.; He, J. Molecular Dynamics Study of Di-CF4 Based Reverse Micelle in Supercritical CO_2. *Phys. Chem. Chem. Phys.* **2016**, *18*, 29156−29163.

(9) Hoefling, T.; Stofesky, D.; Reid, M.; Beckman, E.; Enick, R. M. The Incorporation of a Fluorinated Ether Functionality into a Polymer or Surfactant to Enhance CO_2-Solubility. *J. Supercrit. Fluids* **1992**, *5*, 237−241.

(10) Huang, Z.; Shi, C.; Xu, J.; Kilic, S.; Enick, R. M.; Beckman, E. J. Enhancement of the Viscosity of Carbon Dioxide Using Styrene/Fluoroacrylate Copolymers. *Macromolecules* **2000**, *33*, 5437−5442.

(11) DeSimone, J. M.; Guan, Z.; Elsbernd, C. S. Synthesis of Fluoropolymers in Supercritical Carbon Dioxide. *Science* **1992**, *257*, 945−947.
(12) Cummings, S.; Xing, D.; Enick, R.; Rogers, S.; Heenan, R.; Grillo, I.; Eastoe, J. Design Principles for Supercritical CO_2 Viscosifiers. *Soft Matter* **2012**, *8*, 7044−7055.
(13) Sun, W.; Sun, B.; Li, Y.; Huang, X.; Fan, H.; Zhao, X.; Sun, H.; Sun, W. Thickening Supercritical CO_2 with π-Stacked Co-Polymers: Molecular Insights into the Role of Intermolecular Interaction. *Polymers* **2018**, *10*, 268.
(14) Kilic, S.; Enick, R. M.; Beckman, E. J. Fluoroacrylate-Aromatic Acrylate Copolymers for Viscosity Enhancement of Carbon Dioxide. *J. Supercrit. Fluids* **2019**, *146*, 38−46.
(15) Zaberi, H. A.; Lee, J. J.; Cummings, S. D.; Beckman, E. J.; Enick, R. M.; Dailey, C.; Vasilache, M. *Fluoroacrylate Polymers as CO_2−Soluble Conformance Control Agents*; SPE-190176-MS; Society of Petroleum Engineers, 2019.
(16) Li, Y.; Wang, Y.; Guo, G.; Wang, K.; Gomado, F.; Zhang, C. The effect of fluorocarbon surfactant on the gas-wetting alteration of reservoir. *Pet. Sci. Technol.* **2018**, *36*, 951−958.
(17) Zhang, S.; She, Y.; Gu, Y. Evaluation of Polymers as Direct Thickeners for CO_2 Enhanced Oil Recovery. *J. Chem. Eng. Data* **2011**, *56*, 1069−1079.
(18) Gu, Y.; Zhang, S.; She, Y. Effects of Polymers as Direct CO_2 Thickeners on the Mutual Interactions Between a Light Crude Oil and CO_2. *J. Polym. Res.* **2013**, *20*, 61.
(19) Al Hinai, N. M.; Saeedi, A.; Wood, C. D.; Myers, M.; Valdez, R.; Sooud, A. K.; Sari, A. Experimental Evaluations of Polymeric Solubility and Thickeners for Supercritical CO_2 at High Temperatures for Enhanced Oil Recovery. *Energy Fuels* **2018**, *32*, 1600−1611.
(20) Allen, M. P.; Tildesley, D. J. *Computer Simulation of Molecular Liquids*; Oxford University Press: Oxford, 1987.
(21) Frenkel, D.; Smit, B. *Understanding Molecular Simulation: From Algorithms to Applications*; Academic Press: London, 2002.
(22) Salaniwal, S.; Cui, S. T.; Cochran, H. D.; Cummings, P. T. Molecular Simulation of a Dichain Surfactant/Water/Carbon Dioxide System. 1. Structural Properties of Aggregates. *Langmuir* **2001**, *17*, 1773−1783.
(23) Salaniwal, S.; Cui, S. T.; Cochran, H. D.; Cummings, P. T. Molecular Simulation of a Dichain Surfactant/Water/Carbon Dioxide System. 2. Self-Assembly and Aggregation Dynamics. *Langmuir* **2001**, *17*, 1784−1792.
(24) Senapati, S.; Keiper, J. S.; DeSimone, J. M.; Wignall, G. D.; Melnichenko, Y. B.; Frielinghaus, H.; Berkowitz, M. L. Structure of Phosphate Fluorosurfactant Based Reverse Micelles in Supercritical Carbon Dioxide. *Langmuir* **2002**, *18*, 7371−7376.
(25) Wang, M.; Fang, T.; Wang, P.; Yan, Y.; Zhang, J.; Liu, B.; Sun, X. Molecular-Scale Design of Hydrocarbon Surfactant Self-Assembly in Supercritical CO_2. *Langmuir* **2017**, *33*, 5291−5297.
(26) Wang, M.; Wang, J.; Fang, T.; Yan, Y.; Wang, Z.; Zhang, J. Shape Transition of Water-in-CO_2 Reverse Micelles Controlled by the Surfactant Midpiece. *Phys. Chem. Chem. Phys.* **2018**, *20*, 15535−15542.
(27) Girard, E.; Tassaing, T.; Camy, S.; Condoret, J.-S.; Marty, J.-D.; Destarac, M. Enhancement of Poly(vinyl ester) Solubility in Supercritical CO_2 by Partial Fluorination: The Key Role of Polymer-Polymer Interactions. *J. Am. Chem. Soc.* **2012**, *134*, 11920−11923.
(28) Hoogerbrugge, P. J.; Koelman, J. M. V. A. Simulating Microscopic Hydrodynamic Phenomena with Dissipative Particle Dynamics. *Europhys. Lett.* **1992**, *19*, 155−160.
(29) Español, P.; Warren, P. Statistical Mechanics of Dissipative Particle Dynamics. *Europhys. Lett.* **1995**, *30*, 191−196.
(30) Groot, R. D.; Warren, P. B. Dissipative Particle Dynamics: Bridging the Gap Between Atomistic and Mesoscopic Simulation. *J. Chem. Phys.* **1997**, *107*, 4423−4435.
(31) Huang, L.; Ning, Z.; Wang, Q.; Qi, R.; Li, J.; Zeng, Y.; Ye, H.; Qin, H. Thermodynamic and Structural Characterization of Bulk Organic Matter in Chinese Silurian Shale: Experimental and Molecular Modeling Studies. *Energy Fuels* **2017**, *31*, 4851−4865.
(32) Ungerer, P.; Collell, J.; Yiannourakou, M. Molecular Modeling of the Volumetric and Thermodynamic Properties of Kerogen: Influence of Organic Type and Maturity. *Energy Fuels* **2015**, *29*, 91−105.
(33) Jackson, K.; Bowman, L. E.; Fulton, J. L. Water Solubility Measurements in Supercritical Fluids and High-Pressure Liquids Using Near-Infrared Spectroscopy. *Anal. Chem.* **1995**, *67*, 2368−2372.
(34) Trung, N. T.; Hung, N. P.; Hue, T. T.; Nguyen, M. T. Existence of both Blue-Shifting Hydrogen Bond and Lewis Acid-Base Interaction in the Complexes of Carbonyls and Thiocarbonyls with Carbon Dioxide. *Phys. Chem. Chem. Phys.* **2011**, *13*, 14033−14042.
(35) Marcus, Y. Solubility Parameter of Carbon Dioxide-An Enigma. *ACS Omega* **2018**, *3*, 524−528.
(36) Mishra, V. K.; Temelli, F.; Ooraikul, B. Modeling Binary Phase Behavior of Supercritical Carbon Dioxide and Fatty Acid Esters. *J. Supercrit. Fluids* **1993**, *6*, 51−57.
(37) Mayoral, E.; Nahmad-Achar, E. Multiscale Modeling of the Effect of Pressure on the Interfacial Tension and Other Cohesion Parameters in Binary Mixtures. *J. Phys. Chem. B* **2016**, *120*, 2372−2379.
(38) Bikkina, P. K.; Shoham, O.; Uppaluri, R. Equilibrated Interfacial Tension Data of the CO_2−Water System at High Pressures and Moderate Temperatures. *J. Chem. Eng. Data* **2011**, *56*, 3725−3733.
(39) de Gennes, P. G. *Scaling Concepts in Polymer Physics*; Cornell University Press: New York, 1979.
(40) Le Guillou, J. C.; Zinn-Justin, J. Critical Exponents for the *N*-Vector Model in Three Dimensions from Field Theory. *Phys. Rev. Lett.* **1977**, *39*, 95−98.
(41) Plimpton, S. Fast Parallel Algorithms for Short-Range Molecular Dynamics. *J. Comput. Phys.* **1995**, *117*, 1−19.
(42) Sun, H.; Mumby, S. J.; Maple, J. R.; Hagler, A. T. An ab Initio CFF93 All-Atom Force Field for Polycarbonates. *J. Am. Chem. Soc.* **1994**, *116*, 2978−2987.
(43) Gama Goicochea, A.; Romero-Bastida, M.; López-Rendón, R. Dependence of Thermodynamic Properties of Model Systems on Some Dissipative Particle Dynamics Parameters. *Mol. Phys.* **2007**, *105*, 2375−2381.

DOI: 10.1021/acs.jpcc.9b04293
J. Phys. Chem. C 2019, 123, 17010−17018